

# Pt(II) versus Pt(IV) in Carbene Glycoconjugate Antitumor Agents: Minimal Structural Variations and Great Performance Changes

Alfonso Annunziata, Angela Amoresano, Maria Elena Cucciolo, Roberto Esposito, Giarita Ferraro, Ilaria Iacobucci, Paola Imbimbo, Rosanna Lucignano, Massimo Melchiorre, Maria Monti, Chiara Scognamiglio, Angela Tuzi, Daria Maria Monti,\* Antonello Merlino,\* and Francesco Ruffo\*

Cite This: *Inorg. Chem.* 2020, 59, 4002–4014

Read Online

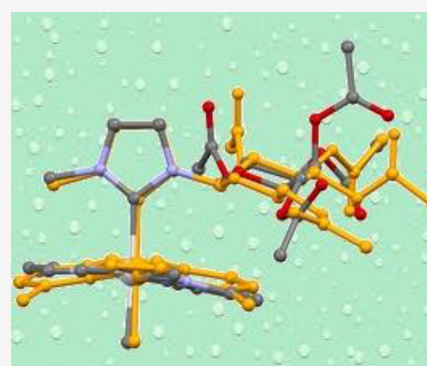
ACCESS |

Metrics & More

Article Recommendations

Supporting Information

**ABSTRACT:** Octahedral Pt(IV) complexes (**2Pt–R**) containing a glycoconjugate carbene ligand were prepared and fully characterized. These complexes are structural analogues to the trigonal bipyramidal Pt(II) species (**1Pt–R**) recently described. Thus, an unprecedented direct comparison between the biological properties of Pt compounds with different oxidation states and almost indistinguishable structural features was performed. The stability profile of the novel Pt(IV) compounds in reference solvents was determined and compared to that of the analogous Pt(II) complexes. The uptake and antiproliferative activities of **2Pt–R** and **1Pt–R** were evaluated on the same panel of cell lines. DNA and protein binding properties were assessed using human serum albumin, the model protein hen egg white lysozyme, and double stranded DNA model systems by a variety of experimental techniques, including UV–vis absorption spectroscopy, fluorescence, circular dichroism, and electrospray ionization mass spectrometry. Although the compounds present similar structures, their in-solution stability, cellular uptake, and DNA binding properties are diverse. These differences may represent the basis of their different cytotoxicity and biological activity.



## INTRODUCTION

The improvement of the anticancer performance of metal-based agents is an important task of modern chemistry.<sup>1</sup> Among the numerous strategies aimed at enhancing both activity and selectivity of these molecules, conjugation with biologically active molecular fragments targeting tumor cells is very promising.<sup>2–8</sup> In this context, our group has recently investigated Pt(II) complexes in 18 e<sup>−</sup> trigonal bipyramidal geometry (*tbp*) containing a sugar-based axial ligand (**1** in Figure 1).<sup>9–12</sup>

This choice simultaneously exploited: (i) the importance of the oxidation state (II), (ii) the stability of the coordinative saturation, and (iii) the possible target recognition of the sugar fragment mediated by the Warburg effect.<sup>13,14</sup> During these

studies, interesting results have been obtained with a cationic complex containing a glucoconjugate carbene (**1Pt–Glu** in Figure 2) that showed a cytotoxic effect on cancer cells 2 orders of magnitude higher than cisplatin. Moreover, a significant selectivity was found for cancer cells (SVT2 and A431) with respect to immortalized cells (BALB/c-3T3 and HaCaT).<sup>11</sup>

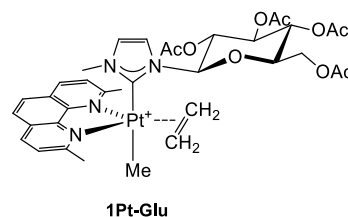


**Figure 2.** Formula of the glucoconjugate *tbp* platinum(II) complex **1Pt–Glu**.

Received: December 19, 2019

Published: March 4, 2020

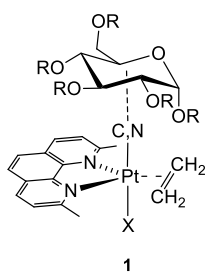


**Figure 1.** Sketch of the glycoconjugate *tbp* platinum(II) complex (**1**).

Other evidence that disclosed straight consequences upon small variations of the coordination environment accompanied this gratifying result: the simple substitution glucose  $\rightarrow$  galactose (epimers at C4) or the removal of the protecting groups rendered the complex significantly less effective. The results were framed in the light of the key-role played by the sugar portion, whose nature and polarity can affect internalization, the metallodrug cellular pathway, and target recognition.<sup>15–17</sup>

Since fine modulations in the chemical properties of the investigated glucoconjugated Pt(II)-based carbene compounds are associated with significant differences in their biological properties, we have planned to verify the consequences of the change in the oxidation state of Pt on the biological activity of these compounds, preparing Pt(IV) analogues. This study allows a rather rare “true” comparison within the Pt(II)/Pt(IV) analogues.<sup>18–21</sup> In fact, while literature data widely demonstrated that Pt(IV) pro-drugs are competitive with Pt(II) agents,<sup>22–37</sup> it should be underlined that the transition to the higher oxidation state involves large structural variations (e.g., from square-planar to octahedral geometry), which makes a direct comparison between analogous Pt(IV) and Pt(II) compounds less homogeneous and more difficult to interpret. Therefore, the availability of species in the two different states of oxidation, but with an overlapping coordination environment, would provide an unprecedented opportunity to fill this gap. Actually, the platinum(II) complexes **1** in *tbp* geometry are expected to share considerable structural aspects with an octahedral platinum(IV) species of type **2** (Figure 3), where

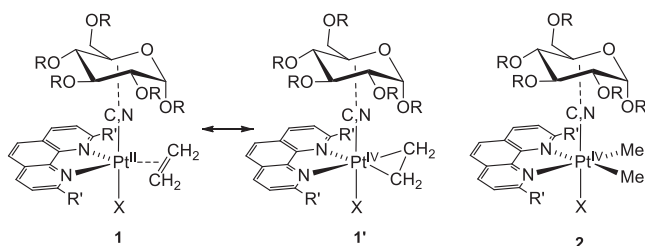


**Figure 3.** Structural analogy between trigonal bipyramidal (**1**) and octahedral (**2**) complexes. This assumption suggested the design of new cationic complexes of Pt(IV) containing two methyl ligands in equatorial positions and the glycoconjugate carbene in one axial site (**2Pt–R** in Figure 4).

two methyl groups substitute ethylene: the structural analogy becomes even more evident considering that the strong Pt-to-ethylene  $\pi$ -backdonation in **1**, typical of trigonal bipyramidal complexes,<sup>38</sup> results in a partial  $sp^2 \rightarrow sp^3$  rehybridization of the alkene carbons, and the whole structure approximates to a Pt(IV)-cyclometallate (**1'**).

In line with the premises, NMR spectroscopy and X-ray diffraction disclosed the stringent structural analogy with the corresponding trigonal bipyramidal Pt(II) species (**1Pt–R**) complexes.<sup>11</sup> Instead, the biological studies revealed deep changes in the cytotoxic properties: **2Pt–Glu** as well as the other Pt(IV) complexes did not show satisfactory activity and selectivity toward cancer cells, confirming that minimal structural variations heavily affect the performance. These conflicting results were a stimulus for a comparative study between **1Pt–Glu** and **2Pt–Glu** to gain insights about the effects of the formal difference in the oxidation state and to

access more information about the mechanisms of action that strongly enhance the biological performance of the former one.

Hence, this work reports synthesis, spectroscopic, and structural characterization of octahedral Pt(IV) complexes (**2Pt–R**; Figure 4), along with a thorough comparative study

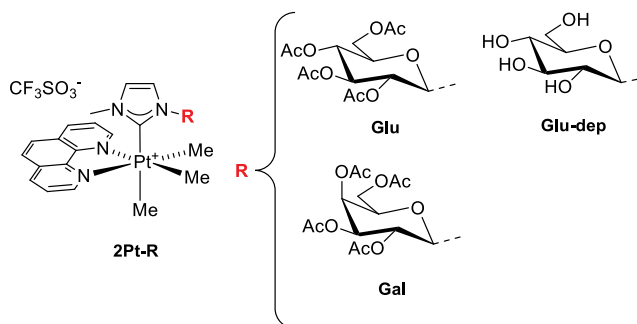


**Figure 4.** Formula of the glucoconjugate octahedral platinum(IV) complexes **2Pt–R**. Labeling of the complexes: Glu = glucose, Gal = galactose, and dep = deprotected.

of their chemical stability in different experimental conditions and of biological properties, comprising cytotoxic activity, cellular uptake, interaction with DNA and proteins.

## RESULTS

**Synthesis and Structural Characterization of Complexes 2Pt–R.** Scheme 1 displays the synthesis of complexes **2Pt–R**. The aquo-precursor **2Pt–H<sub>2</sub>O** was obtained by suspending **2Pt–I** in a solution containing silver triflate in acetone or methanol. The precipitated AgI was filtered off, and an equivalent of the appropriate silver carbene **R–Ag–Br** was added to the solution. The mixture was stirred for 3 days in acetone or in methanol. The precipitated AgBr was removed by filtration, and the **2Pt–R** complexes were crystallized, either with the hydroxyls in acetylated form, when the reaction was carried out in acetone, or deprotected, when the solvent was methanol. In this second case, the acetyl groups undergo transesterification catalyzed by the Lewis acidity of the Ag(I) ion present in the reaction system.

The complexes display octahedral geometry with the equatorial plane defined by the bidentate ligand 1,10-phenanthroline (phen) and two methyls, while the axial positions are occupied by the carbene and a third methyl. The presence of phen represents the second minimal difference with respect to **1Pt–R** complexes, which contain 2,9-dimethyl-1,10-phenanthroline (dmphen), which is necessary to ensure the stability of the *tbp* geometry. Attempts to introduce dmphen in type **2** complexes did not produce satisfactory results.

The complexes were characterized by NMR spectroscopy (Figures S1–S4) and X-ray diffraction (Table S1 and Figures S5–S9). The following observations contributed to the characterization of the complexes: a singlet close to  $\delta$  0 and two singlets around  $\delta$  1.5, attributable, respectively, to the axial methyl and to the two nonequivalent equatorial methyls, with the satellites due to coupling to <sup>195</sup>Pt; the multiplets of the sugar protons with the expected coupling constants; two singlets at ca.  $\delta$  7 for the protons riding on the carbene ligand. The signals were practically coincident with the corresponding ones of **1Pt–R** complexes (Figure 5). The Pt–C (carbene)

## Scheme 1. Synthesis of Complexes of Type 2Pt–R

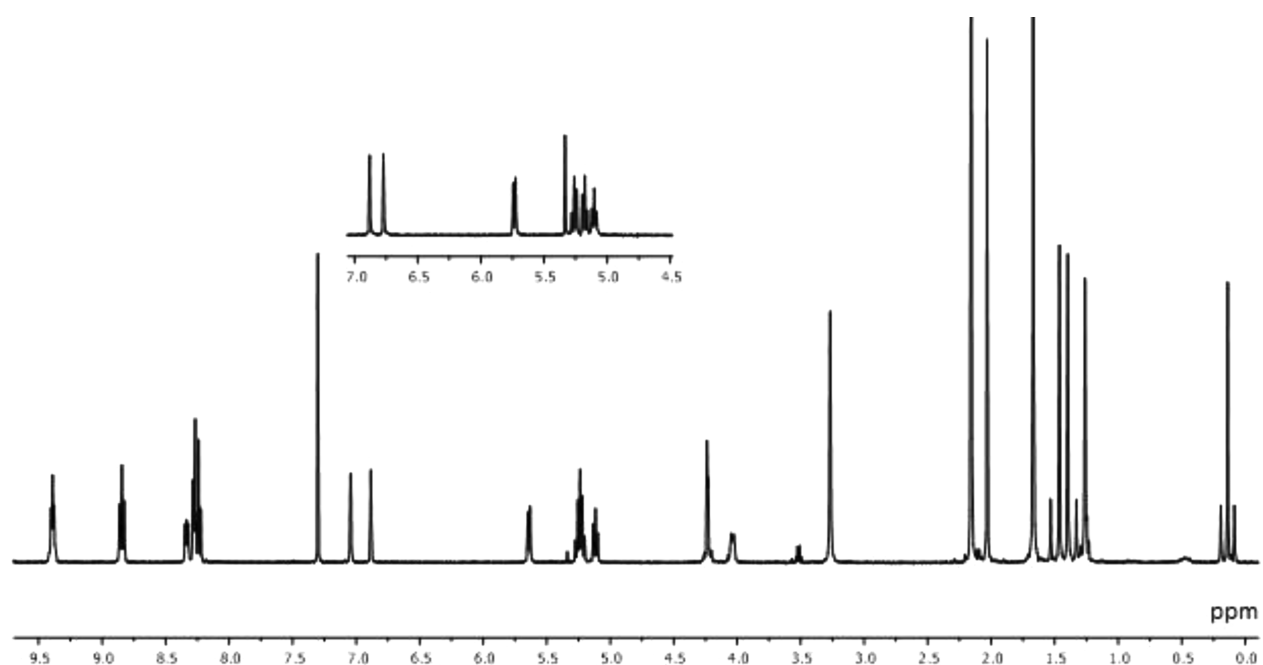
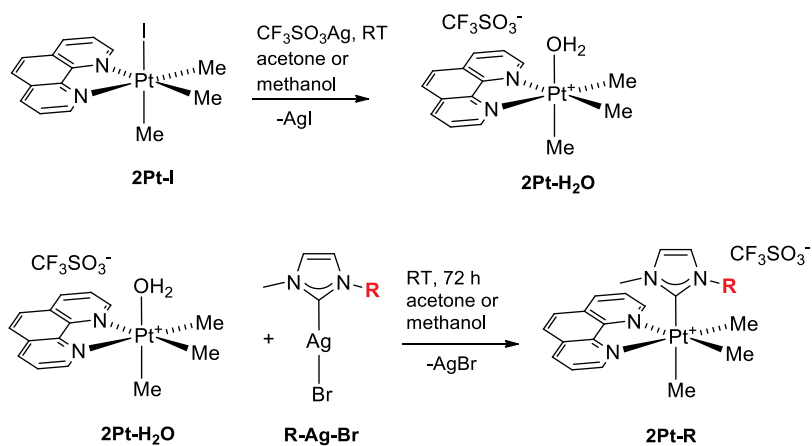


Figure 5.  $^1\text{H}$  NMR spectrum of  $2\text{Pt-Glu}$  in  $\text{CDCl}_3$  at 298 K. The inset shows the corresponding portion of  $1\text{Pt-Glu}$ .

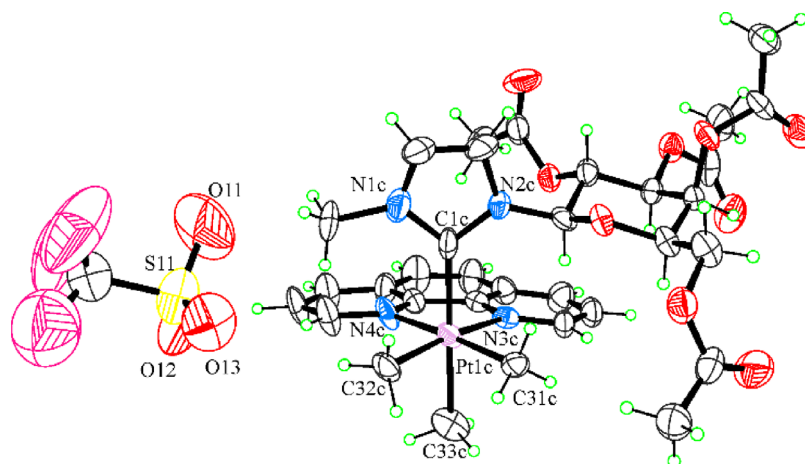
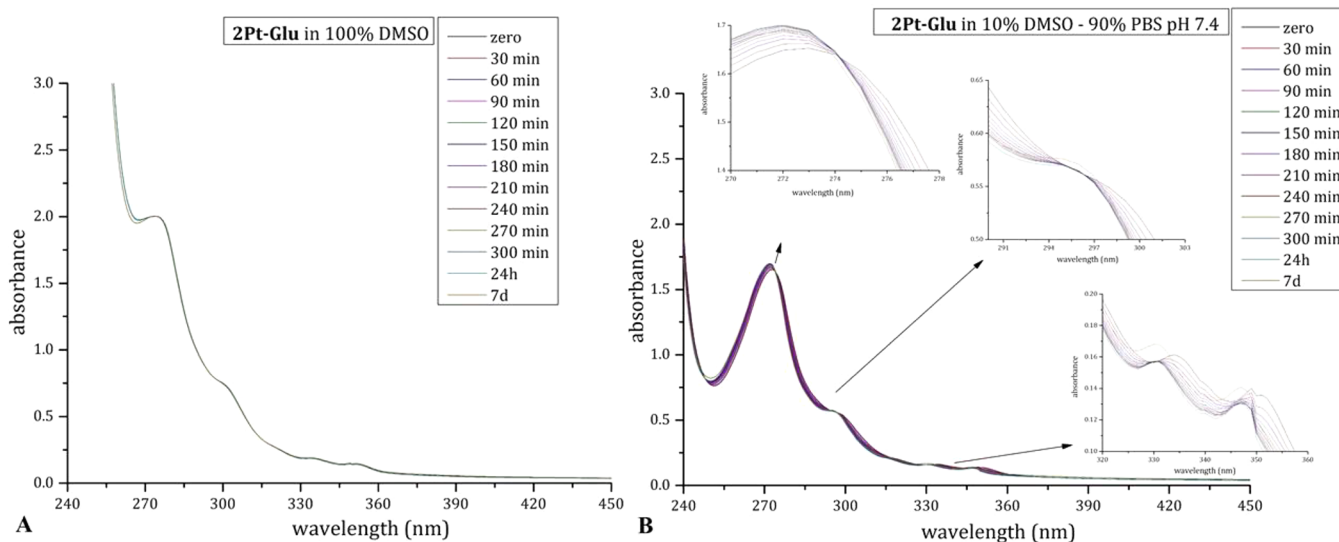


Figure 6. ORTEP view of one of the four independent molecules of  $2\text{Pt-Gal}$ . Thermal ellipsoids are drawn at a 30% probability level.

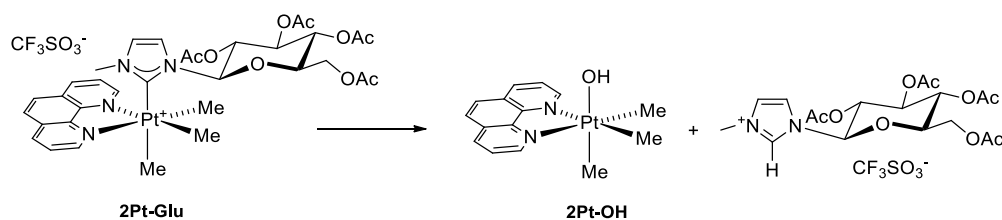
resonances were found at the expected frequencies in the carbon spectra ( $^1J_{\text{Pt-C}}$  ca. 600 Hz).

The single crystal X-ray analysis confirmed that compound  $2\text{Pt-Gal}$  contains a cationic carbene complex of Pt(IV) with



**Figure 7.** Time course UV-vis spectra of 50  $\mu\text{M}$  **2Pt-Glu** in 100% DMSO (A) and 10% DMSO/90% PBS (pH 7.4) (B). In (B), details of the isosbestic points are also shown.

### Scheme 2. Hydrolysis of **2Pt-Glu**



$\text{CF}_3\text{SO}_3^-$  (triflate) as counterion. The structure of **2Pt-Gal** is reported in Figure 6. Details of the structural analysis are reported in the Supporting Information.

The compound crystallizes in the triclinic *P1* space group with four independent pairs of cations and anions in the unitary cell. All bond lengths and angles are in the expected range. No significant differences in the geometric parameters were found between the four independent pairs of molecular ions; only one pair is reported in Figure 6. The Pt atom adopts a fairly regular octahedral geometry with the bidentate phen ligand and two methyl groups in the equatorial plane. The two Pt–Me distances (2.05(2) and 2.07(2) Å) are in line with previous literature data.<sup>39</sup> The axial positions are occupied by the central carbon atom of the carbene ligand and by a third methyl group. The crystal structure of **2Pt-Gal** revealed a close analogy with **1Pt-Glu** reported previously.<sup>11</sup> Despite the different oxidation state of platinum, the coordination environment in **2Pt-Gal** overlaps well with that observed in the structure of **1Pt-Glu**. The glycoconjugate carbene groups also overlap well, apart from the changed axial or equatorial position in the ring. The galactosyl group at the N2 atom is in the usual chair conformation with three equatorial and one axial substituents. At variance with **1Pt-Glu**, a not flat shape is adopted by the galactosyl group due to the axial substituent that is placed far away from the phen ligand plane to avoid steric effects. A less evident bowl-like distortion of the phen bidentate ligand is observed with respect to **1Pt-Glu**, with the dihedral angle between the mean planes of the outer rings ranging from 8(2)° to 11(2)° in the four independent cations. In the crystal, the triflate anions are placed in the neighborhood of Pt(IV), with a mean Pt...O (triflate) distance

of 5.91(3) Å. The crystal packing is dominated by electrostatic interactions and is also stabilized by weak C–H...O interactions.

**In-Solution Studies.** Relevant aspects of the in-solution behavior of **2Pt-Glu** were studied by <sup>1</sup>H NMR and UV-vis absorption spectroscopy in comparison to **1Pt-Glu**.<sup>11</sup> UV-vis spectra of **2Pt-Glu** were recorded in aqueous media (10% DMSO/90% PBS (pH 7.4) and 50% DMSO/50% PBS (pH 7.4)) and pure DMSO and reported in Figures 7A,B and S10. Interestingly, **1Pt-Glu** and **2Pt-Glu** showed very different stabilities. **1Pt-Glu** is stable in aqueous media, while it exchanges ethylene and dmphen ligands for a solvent molecule in pure DMSO.<sup>11</sup> On the contrary, **2Pt-Glu** does not show appreciable changes in pure DMSO, while it undergoes spectral changes with time in aqueous media. The presence of isosbestic points in the spectral profiles of **2Pt-Glu** in mixed DMSO/PBS solutions (Figures 7B and S10) confirmed the occurrence of a ligand exchange process.

Similar results were observed by <sup>1</sup>H NMR. The analysis of the NMR spectra in 10% DMSO/90% PBS (pH 7.4) indicates that **2Pt-Glu** undergoes hydrolysis of the carbene moiety, yielding a hydroxyl Pt species (**2Pt-OH** in Scheme 2) and the imidazolium salt.<sup>40–42</sup> The process is complete within 24 h (Figure S11). The two products were identified by comparing their NMR spectra with those of authentic samples. An influence of pH was observed; as in D<sub>2</sub>O, the same process occurred slowly. On the other hand, **1Pt-Glu** is stable over days under the same experimental conditions.<sup>11</sup>

**Interaction with DNA.** The interaction of **2Pt-Glu** with DNA was studied by fluorescence, circular dichroism, electro-

spray ionization mass spectrometry, and  $^1\text{H}$  NMR, in comparison to that of **1Pt-Glu**.<sup>11</sup>

The binding of **2Pt-Glu** to calf-thymus DNA (ctDNA) was first evaluated by using the ethidium bromide (EtBr) displacement fluorescence assay (Figure S12). Results of the fluorescence assay indicate that **2Pt-Glu** does not displace EtBr from the ctDNA major groove, as is observed also in the case of **1Pt-Glu** and differently from cisplatin and the dmphen ligand.<sup>11</sup>

Then, CD spectra of ctDNA in the presence of **2Pt-Glu** in different molar ratios were registered and compared to the spectrum of drug-free DNA (Figure 8).

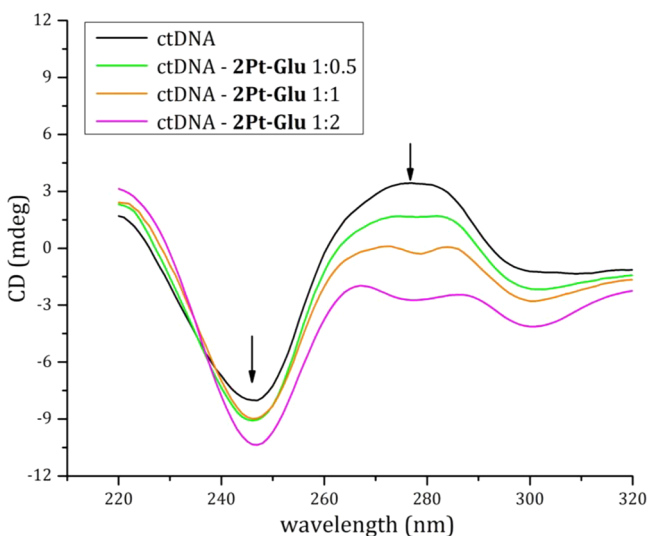


**Figure 8.** CD spectra of ctDNA ( $200\ \mu\text{M}$  in  $0.01\ \text{M}$  ammonium acetate buffer, pH 7.5) in the absence (black line) and in the presence of **2Pt-Glu** with different DNA to metal molar ratios (1:0.5 green line, 1:1 orange line, and 1:2 purple line).

The CD spectra of ctDNA present the typical features of the right-handed B form of DNA, in agreement with literature data.<sup>11</sup> In the presence of **2Pt-Glu**, the intensities of both positive and negative bands shift to lower ellipticity values, as is observed for **1Pt-Glu**.<sup>11</sup>

Successively, to shed light on the binding of the two compounds to a DNA model system at molecular level, the binding of **1Pt-Glu** and **2Pt-Glu** to a 20 mer double stranded oligonucleotide (dsDNA) was investigated by electrospray mass spectrometry. ESI-MS spectra of **1Pt-Glu** and **2Pt-Glu** are reported in Figure 9A,B, respectively, and all signals detected are summarized in Table 1. In both cases, one molecule of each Pt compound binds the dsDNA, as demonstrated by the presence of the species at molecular weights of  $13\ 096.53 \pm 2.20\ \text{Da}$  and  $13\ 071.34 \pm 0.87\ \text{Da}$  (Table 1), ascribable to dsDNA bound to one molecule of **1Pt-Glu** and one of **2Pt-Glu**, respectively (Figure 9).

These data suggest that the Pt compounds share common features in binding the dsDNA. Moreover, the behavior of the two molecules is different from that observed in the reaction of the same DNA model system with cisplatin. Indeed, when the dsDNA was incubated with cisplatin, under the same experimental conditions, up to three cisplatin molecules bound the dsDNA. However, upon binding, each cisplatin molecule lost both  $\text{Cl}^-$  ligands, and some of them were replaced by other fragments (i.e., acetate ions, Figure S13 and Table S1).

From these data, it appears that **2Pt-Glu** is more stable in aqueous media in the presence of DNA. ESI spectra also revealed a difference in the binding affinity of **1Pt-Glu** and **2Pt-Glu** toward ssDNA. In the case of **2Pt-Glu**, two additional peaks were detected at  $6817.08 \pm 0.46$  and  $7087.04 \pm 0.42\ \text{Da}$  (Figure 9B). These peaks are indicative of a partial binding of **2Pt-Glu** to ssDNA. This ssDNA is in equilibrium with dsDNA and is already detectable in the ESI spectrum in the absence of **2Pt-Glu** (data not shown). No additional peaks were observed in the ESI spectra collected upon incubation of **1Pt-Glu** with dsDNA under the same experimental conditions.

To further confirm that DNA was able to increase the stability of the Pt compounds, a time course in the UV-vis spectra of **2Pt-Glu** and **1Pt-Glu** in the presence of DNA was performed (Figure 10). The UV-vis spectra remain unchanged during the time course, with a minimal shift of the maximum absorption peak from 273 to 270 nm observed only after 7 days. This experiment confirmed that **2Pt-Glu** is more stable in aqueous media in the presence of DNA.

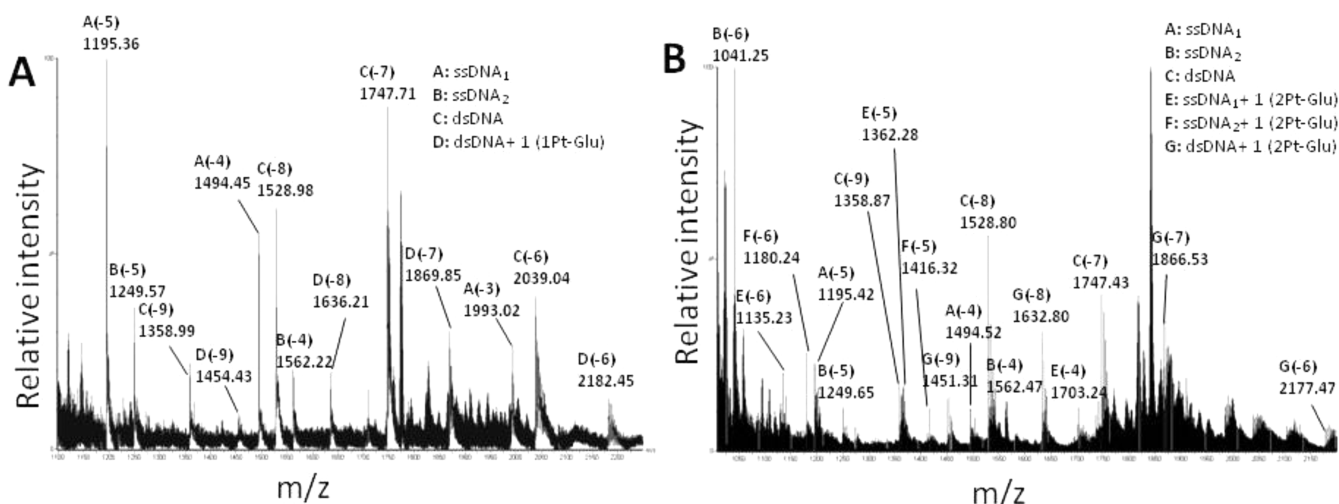


**Figure 9.** ESI-MS spectra of dsDNA incubated with (A) **1Pt-Glu** and (B) **2Pt-Glu**.

Table 1. Results of ESI-MS Analysis of Species Formed upon Reaction of DNA with 1Pt-Glu and 2Pt-Glu<sup>a</sup>

metal complex	signal ( <i>m/z</i> )	signal charge	exp MW (Da)	theoretical MW (Da)	species
1Pt-Glu	1195.36	A (-5)	5982.92 ± 0.80	5983.9	ssDNA <sub>1</sub>
	1494.45	A (-4)			
	1993.02	A (-3)			
	1249.57	B (-5)	6254.45 ± 0.50	6255.1	ssDNA <sub>2</sub>
	1562.22	B (-4)			
	1358.99	C (-9)	12240.33 ± 0.30	12239	dsDNA
	1528.98	C (-8)			
	1747.71	C (-7)			
	2039.04	C (-6)			
	1454.43	D (-9)	13096.53 ± 2.20	13097.8	dsDNA + 1 (1Pt-Glu)
	1636.21	D (-8)			
	1869.85	D (-7)			
	2182.45	D (-6)			
1195.42	A (-5)	5982.15 ± 0.03			
1494.52	A (-4)				
1041.25	B (-6)		6253.58 ± 0.27	6255.1	ssDNA <sub>2</sub>
1249.65	B (-5)				
1562.47	B (-4)	12238.82 ± 0.27	12239	dsDNA	
1358.87	C (-9)				
1528.80	C (-8)				
1747.43	C (-7)				
1135.23	E (-6)	6817.08 ± 0.46	6816.15	ssDNA <sub>1</sub> + 1 (2Pt-Glu)	
1362.28	E (-5)				
1703.24	E (-4)				
1180.24	F (-6)	7087.04 ± 0.42	7087.35	ssDNA <sub>2</sub> + 1 (2Pt-Glu)	
1416.32	F (-5)				
1451.31	G (-9)	13071.34 ± 0.87	13071.3	dsDNA + 1 (2Pt-Glu)	
1632.80	G (-8)				
1866.53	G (-7)				

<sup>a</sup>The *m/z* values detected in MS spectra and their relative charges as well as experimental (exp) and theoretical (theor) monoisotopic mass values and the corresponding ion species are reported. dsDNA = double stranded DNA; ssDNA = single stranded DNA.

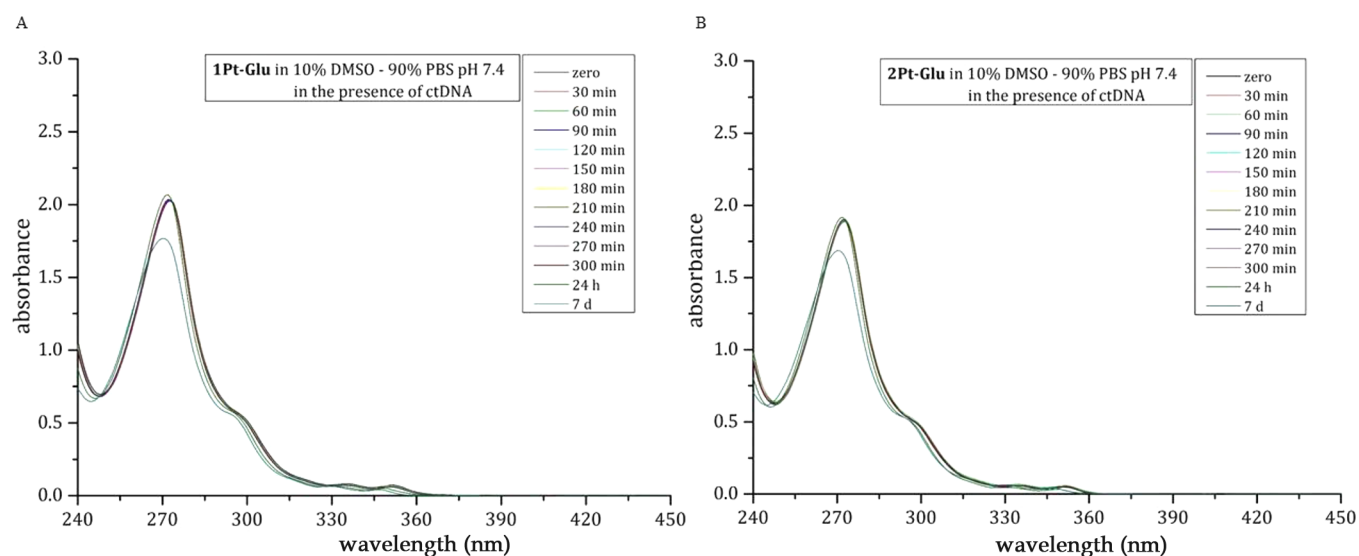
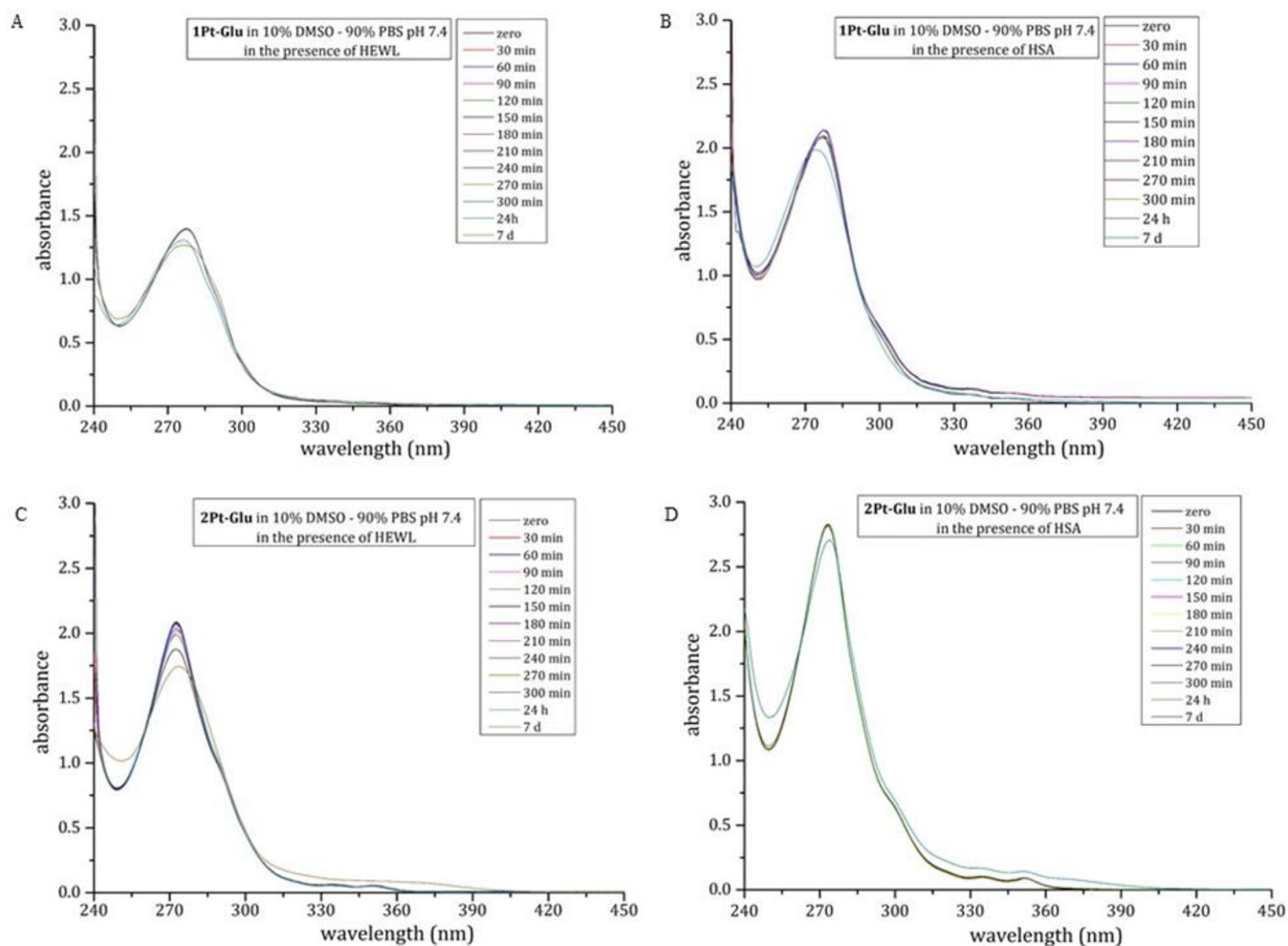


Figure 10. Time course UV-vis spectra of 50  $\mu$ M 1Pt-Glu (A) and 50  $\mu$ M 2Pt-Glu (B) in 10% DMSO/90% PBS (pH 7.4) in the presence of ctDNA.

Finally, to obtain further insights into the reactivity of the complexes with DNA, the interaction of 1Pt-Glu and 2Pt-Glu with 2-deoxyguanosine monophosphate (dGMP) was investigated by <sup>1</sup>H NMR. 1Pt-Glu and 2Pt-Glu were incubated at 37 °C for up to 2 weeks in PBS 90% (pH 7.4)/DMSO 10%, and spectra were recorded at different times

of incubation. Under these conditions, the coordination of guanosine was not observed.

**Interactions with Proteins.** The possible interaction of 1Pt-Glu and 2Pt-Glu with the model protein hen egg white lysozyme (HEWL) and with human serum albumin (HSA) was then studied by UV-vis absorption spectroscopy and



**Figure 11.** Time course UV-vis spectra of 50  $\mu\text{M}$  1Pt-Glu (A, B) and 50  $\mu\text{M}$  2Pt-Glu (C, D) in 10% DMSO/90% PBS (pH 7.4) in the presence of HEWL (A, C) and HSA (B, D) at a 1:3 protein to metal molar ratio.

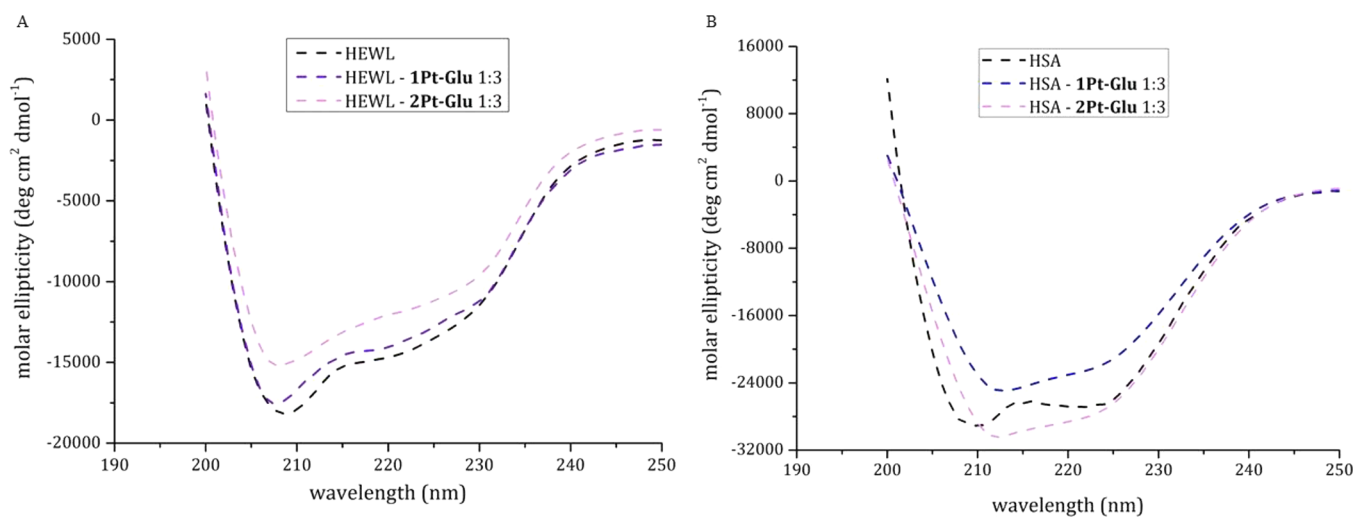


**Figure 12.** Far UV-CD spectra of HEWL (A) and HSA (B) incubated for 24 h in the presence of 1Pt-Glu (dark purple/blue dashed curve/spectrum) and 2Pt-Glu (light purple dashed curve/spectrum) in 10% PBS (pH 7.4) at a 1:3 protein to metal molar ratio. Free protein is represented by black dashed curves/spectra. (Protein concentration 0.10 mg/mL).

circular dichroism. UV-vis spectra of the two compounds in the absence and in the presence of HEWL and HSA were collected over 7 days under different experimental conditions (Figures 11 and S14).

The analysis of the spectral profiles shows that both 1Pt-Glu and 2Pt-Glu are rather stable in the presence of the two proteins. The comparison between these spectra and those collected for the compounds in the absence of the proteins

**Table 2.** IC<sub>50</sub> Values (μM) Obtained for Pt Compounds on A431, SVT2, BALB/c-3T3, and HaCaT Cells after 48 h of Incubation<sup>a</sup>

cell line	2Pt–Glu	2Pt–Glu–dep	2Pt–Gal	2Pt–OH	1Pt–Glu <sup>11</sup>	cisplatin <sup>11</sup>
HaCaT	43.8 ± 4.3	55 ± 9	>125	13.6 ± 1.6	13 ± 1.7	6.6 ± 0.3
A431	43.8 ± 2.8	41.8 ± 1.7	>125	14.9 ± 0.6	0.40 ± 0.01	39 ± 12
BALB/c-3T3	196 ± 14	59.6 ± 2.6	>125	7.2 ± 0.7	6.3 ± 0.4	240 ± 47
SVT2	176 ± 13	122 ± 5	>125	6.4 ± 0.6	0.65 ± 0.07	195 ± 7

<sup>a</sup>The IC<sub>50</sub> values for 1Pt–Glu and cisplatin are from ref 11.

(Figure 7) indicates that the incubation of 2Pt–Glu with HEWL or with HSA increases the in-solution stability of this metalloglu in the aqueous media, in agreement with what is observed in the presence of DNA.

To evaluate in detail the potential interaction of 1Pt–Glu and 2Pt–Glu with HEWL and HSA, the secondary structure content of the two proteins was evaluated by CD spectroscopy at increasing concentrations of the metal compounds. Far UV-CD spectra were collected upon 24 h of incubation at room temperature. CD spectra reported in Figure 12 show a decrease of the molar ellipticity at increasing concentrations of 1Pt–Glu and 2Pt–Glu for both HEWL and HSA. This is indicative of a potential binding of the Pt compounds to the proteins.

**Cytotoxicity and Cellular Uptake Experiments.** Finally, in order to inspect any biological difference between 1Pt–Glu and 2Pt–Glu, the cytotoxicity of 2Pt–Glu and its derivatives was assessed by the MTT assay. The same panel of cells used to study the biological activity of 1Pt–Glu were used. Cells were incubated with increasing concentrations of the Pt compounds, and then, cell survival was evaluated after 48 h of incubation. The IC<sub>50</sub> values are reported in Table 2, and the results previously obtained with 1Pt–Glu and cisplatin are reported for comparison.<sup>11</sup> No cytotoxic activity was reported for 2Pt–Gal, up to 125 μM, evidencing a close analogy with its analogue 1Pt–Gal, which was considerably less active and selective than 1Pt–Glu.<sup>11</sup> These data suggest that the cytotoxic activity of these classes of compounds (1Pt–R and 2Pt–R) is strictly dependent on the sugar portion and very sensible upon its small variations. Surprisingly, 2Pt–Glu showed a completely different behavior with respect to 1Pt–Glu, as it was about 100 times less toxic than 1Pt–Glu and it completely lost its selectivity for the cancer cells analyzed. As 2Pt–Glu can be hydrolyzed in aqueous buffer to form 2Pt–OH, the latter compound was tested for its cytotoxicity. 2Pt–OH was found to be more toxic than 2Pt–Glu on immortalized cells, but still no selectivity was observed.

Thus, a different mechanism of action occurring between the two drugs was hypothesized, and their uptake in A431 cells was analyzed. Cancer cells were incubated with either 1Pt–Glu or 2Pt–Glu at the concentrations needed to reach the IC<sub>50</sub> values. Cisplatin was used as a reference. After a 48 h incubation, the Pt content was measured by ICP-MS. The amount of Pt uptake in A431 cells was 0.65 ± 0.15% for 1Pt–Glu with respect to 0.39 ± 0.09% for 2Pt–Glu and 0.79 ± 0.25% for cisplatin. These data indicate that in the case of 1Pt–Glu the percentage of Pt internalized by the cells is about 2 times higher than that found in the case of the cells treated with 2Pt–Glu. Noteworthy, in the case of 1Pt–Glu, the amount of Pt needed to reach the IC<sub>50</sub> is about 100 times lower than that needed with 2Pt–Glu.

**Attempts to Reduce 2Pt–Glu In Vitro.** To explain the decrease in the cytotoxic activity observed for 2Pt–R

compared to 1Pt–R, we focused on the activation of Pt(IV) prodrugs, which are known to undergo a reduction in the biological environment, releasing the Pt(II) active species.<sup>30,43</sup>

In vitro reduction was attempted using ascorbic acid and glutathione, which are the most abundant reducing agent in intracellular media. 2Pt–Glu (1 mM) was incubated at 37 °C in 90% PBS (pD 7.4)/10% DMSO with different excesses (2–25 mM) of the reducing agent, and <sup>1</sup>H NMR spectra were recorded at different times of incubation. In these conditions, no sign of reduction was observed for 2Pt–Glu or for its hydrolysate form 2Pt–OH (Scheme 2). Furthermore, no coordination of glutathione ligands was observed, despite the known ability of sulfur ligands to coordinate in the axial positions of coordinatively saturated complexes.<sup>44</sup>

The lack of chemical reduction of 2Pt–Glu and 2Pt–OH is in agreement with the positions of their reduction peaks in the cyclic voltammograms, which are significantly more negative than those of Pt(IV) complexes containing chloride, acetate, or hydroxide ligands.<sup>45</sup> In DMSO, peaks of reduction were observed at –1.54 and –1.89 V for 2Pt–Glu and –1.40, –1.59, and –1.89 V for 2Pt–OH (Figures S15 and S16 and Table S3). This trend is in accord with those observed for organometallic Pt(IV) compounds containing aryl substituents, which do not undergo chemical reduction as well.<sup>46</sup>

## DISCUSSION

Recently, we described novel five-coordinate Pt(II) compounds bearing glycoconjugate carbene ligands, which were characterized and evaluated as potential anticancer compounds in vitro.<sup>11</sup> One of these agents (1Pt–Glu in Figure 2) showed promising in vitro cytotoxic activity and high selectivity toward malignant cells. Since fine variations in its structure were associated with significant differences in the biological properties, we were also intrigued to assess the influence of the oxidation state of the metal, another factor of great impact on the biological properties of the complexes. The starting point of the present work was that the effect of the metal oxidation state could be assessed only with other structural aspects being equal. This perspective cannot be easily realized if the comparison regards the Pt(II)/Pt(IV) couple, by virtue of the different coordination geometries that these ions typically assume in their complexes. In this work, the target was achieved by exploiting the analogy between the cyclopropametallate fragment, typical of the Pt(II)–ethene bond, and the (bis-methyl)Pt(IV) moiety. The introduction of these motifs in the equatorial plane of trigonal bipyramidal and octahedral species (Figure 3) offers the unprecedented possibility of making a homogeneous comparison between Pt(II) and Pt(IV) compounds (1Pt–R and 2Pt–R, respectively) regarding spectroscopic and structural features, solution stability, biological properties, and the ability to interact with macromolecules.

The experimental data illustrated in this work disclose relevant analogies and differences between the two classes. In full agreement with the initial expectations, their structures are nearly superimposable, and the close similarity of the NMR signals (Figure 5) confirms the similitude between the coordination environments. This returns a practically coincident molecular volume, despite the different oxidation state. However, this latter difference clearly reflects the insolubility behavior: only **1Pt–Glu** is sensitive<sup>11</sup> to DMSO, a coordinating aprotic solvent, probably due to the aptitude of the equatorial neutral ligand ethene to act as a leaving group. The situation is reversed in the presence of water, a weaker ligand for platinum with respect to DMSO. In this condition, the Pt(IV)–carbene bond of **2Pt–Glu** is responsive (Scheme 2). It is plausible that the high formal charge present on the metal center favors the attack of OH<sup>−</sup> ions that replace the hydrocarbyl ligand. This result is consistent with the poor selectivity toward cancer cells of **2Pt–Glu**, as the loss of the sugar fragment can have important effects on the internalization of the complex.

The stability of **1Pt–Glu** and **2Pt–Glu** toward hydrolysis is enhanced by ct-DNA and proteins: in the presence of these macromolecules, we had no evidence of structural variations of the complexes (Figures 10 and 11). Furthermore, both complexes retain their identity when interacting with DNA (Table 1), while cisplatin undergoes substitution of one chloride for other ligands. This finding confirms the higher general stability of coordinatively saturated species with respect to cisplatin. Although the two compounds show a diverse preference between the single and double strand of DNA, this difference does not offer the cue to clarify the clear difference in activity. A possible explanation can be found first by considering the different degree of internalization displayed by the complexes. The percentage of cellular uptake of **2Pt–Glu** is lower than that of either **1Pt–Glu** or cisplatin. This limitation is accompanied by the stability of the Pt(IV) complex in the presence of either glutathione or ascorbate, which are used on a regular basis to verify the tendency of platinum(IV) complexes to undergo reduction.<sup>43</sup> These literature studies, carried out mainly on complexes containing Pt–Cl bonds, hypothesize that the efficient reduction occurs upon the formation of chloride bridges with the reductant, an event that neither **2Pt–Glu** nor its hydrolysis product **2Pt–OH** (Scheme 2) can give rise to. Therefore, on the basis of the established supposition that Pt(IV) agents need reduction to be effective, it can be assumed that another major reason for the poor activity of **2Pt–Glu** is the lack of reduction in the cytosolic environment; thus, no active species are able to initiate the cytotoxic process.

## EXPERIMENTAL SECTION

Reagents and solvents were purchased from Sigma-Aldrich and were used without further purification. NMR spectra were acquired on a 400 Bruker Avance Ultrashield 400 and on a 500 Varian Inova, located at the Dipartimento di Scienze Chimiche, Università di Napoli Federico II, Napoli (Italy). The solvents were CDCl<sub>3</sub> (CHCl<sub>3</sub>, δ 7.26, and <sup>13</sup>CDCl<sub>3</sub>, δ 77.0, as internal standards), (CD<sub>3</sub>)<sub>2</sub>SO ((CD<sub>2</sub>H)<sub>2</sub>SO), δ 2.49, as internal standard), D<sub>2</sub>O (HDO, δ 4.80 as internal standard), and CD<sub>3</sub>OD (CD<sub>2</sub>HOD, δ 3.30, <sup>13</sup>CD<sub>3</sub>OD, δ 49.0, and <sup>195</sup>PtCl<sub>6</sub><sup>2−</sup>, δ 0, as internal standards). The following abbreviations were used for describing NMR multiplicities: s, singlet; d, doublet; dd, double doublet; triplet; app, apparent; m, multiplet; ABq, AB quartet; Me, methyl. Electrochemical measurements were recorded on a Reference 3000 Gamry instrument controlled by

Framework software. Data analyses were performed with EChem Analyst electrochemical software. Precursors **2Pt–I**,<sup>47</sup> **Glu–Ag–Br**,<sup>48,49</sup> and **Gal–Ag–Br**<sup>11</sup> were synthesized as described in the literature.

**Synthesis of 2Pt–Glu and 2Pt–Gal.** The precursor **2Pt–I** (0.140 g, 0.256 mmol) was suspended into a solution of silver triflate (0.066 g, 0.256 mmol) in acetone (8 mL). After 10 min of stirring, AgI was filtered off on Celite. The filtrate was added to a solution of the appropriate **R–Ag–Br** (0.153 g, 0.256 mmol) in acetone (2 mL). The mixture was stirred and protected from light for 3 days at RT. Then, solid was filtered off, and the solvent was removed under vacuum, yielding a yellow oil. The product was obtained purified by SiO<sub>2</sub> chromatography using 97:3 dichloromethane/methanol. **2Pt–Glu**: (yield 96%) <sup>1</sup>H NMR, CDCl<sub>3</sub>, δ: 9.36 (m, 2H, H-2 phen and H-9 phen), 8.81 (d, 2H, H-4 and H-7 phen), 8.29 (dd, 1H, H-3 or H-8 phen), 8.24 (dd, 1H, H-8 or H-3 phen), 8.22 (ABq, 2H, H-5 and H-6 phen), 7.00 (d, 1H, H-4 or H-5 imidazole), 6.82 (d, 1H, H-5 or H-4 imidazole), 5.58 (d, 1H, *J*<sub>H1–H2</sub> = 8.6 Hz, H-1 glucose), 5.18 (m, 2H, H-2 and H-3 glucose), 5.06 (t, 1H, *J*<sub>H4–H3</sub> = 9.8 Hz, H-4 glucose), 4.20 (m, 2H, H-6 and H-6′ glucose), 4.01 (m, 1H, H-5 glucose), 3.23 (s, 3H, Me imidazole), 2.11 (s, 3H, OAc), 2.10 (s, 3H, OAc), 1.98 (s, 3H, OAc), 1.20 (s, 3H, OAc), 1.41 (s, 3H, <sup>2</sup>*J*<sub>Pt–H</sub> = 70 Hz), 1.34 (s, 3H, <sup>2</sup>*J*<sub>Pt–H</sub> = 70 Hz), 0.08 (s, 3H, <sup>2</sup>*J*<sub>Pt–H</sub> = 55 Hz). <sup>13</sup>C NMR, CDCl<sub>3</sub>, δ: 173.1 (*J*<sub>Pt</sub> = 648 Hz), 170.5, 169.8, 169.5, 168.2, 148.0, 147.6, 146.0, 140.0, 139.4 (×2), 131.8 (×2), 128.9, 128.2, 126.7, 126.3, 125.3, 120.8 (q *J*<sub>C–F</sub> = 322 Hz), 117.9, 83.7, 74.5, 72.4, 69.0, 68.2, 65.9, 61.6, 37.7, 20.7, 20.6, 20.4, 19.8, 5.3 (*J*<sub>Pt</sub> = 506 Hz), −6.1 (*J*<sub>Pt</sub> = 664 Hz), −6.8 (*J*<sub>Pt</sub> = 664 Hz). <sup>195</sup>Pt NMR, CD<sub>3</sub>OD, δ: −2777. Anal. Calcd (found): (C<sub>34</sub>H<sub>41</sub>F<sub>3</sub>N<sub>4</sub>O<sub>12</sub>PtS): C, 41.59 (41.81); H, 4.21 (4.26); N, 5.71 (5.67). **2Pt–Gal** (yield 98%) <sup>1</sup>H NMR, CDCl<sub>3</sub>, δ: 9.34 (m, 2H, H-2 and H-9 phen), 8.84 (m, 1H, H-4 or H-7 phen), 8.80 (m, 1H, H-7 or H-4 phen), 8.28 (dd, 1H, H-3phen or H-8 phen), 8.24 (dd, 1H, H-8 or H-3 phen), 8.22 (s, 2H, H-5 and H-6 phen), 7.07 (d, 1H, H-4 or H-5 imidazole), 6.86 (d, 1H, H-5 or H-4 imidazole), 5.53 (d, 1H, *J*<sub>H1–H2</sub> = 9.4 Hz, H-1 galactose), 5.49 (d, 1H, *J*<sub>H4–H3</sub> = 3.2 Hz, H-4 galactose), 5.39 (t, 1H, *J*<sub>H2–H3</sub> = 9.4 Hz H-2 galactose), 5.02 (dd, 1H, H-3 galactose), 4.13 (m, 2H, H-5 and H-6 galactose), 4.03 (m, 1H, H-6′ galactose), 3.20 (s, 3H, Me imidazole), 2.18 (s, 3H, OAc), 2.10 (s, 3H, OAc), 1.97 (s, 3H, OAc), 1.41 (s, 3H, <sup>2</sup>*J*<sub>Pt–H</sub> = 58 Hz), 1.36 (s, 3H, <sup>2</sup>*J*<sub>Pt–H</sub> = 88 Hz), 1.31 (s, 3H, OAc), 0.06 (s, 3H, <sup>2</sup>*J*<sub>Pt–H</sub> = 55 Hz). <sup>13</sup>C NMR, CDCl<sub>3</sub>, δ: 172.9 (*J*<sub>Pt</sub> = 640 Hz), 170.5, 169.9, 169.7, 168.4, 148.5, 147.8, 146.0, 139.7, 139.5, 131.8, 128.9 (×2), 128.3 (×2), 126.4, 126.2, 125.3, 124.0 (q *J*<sub>C–F</sub> = 327 Hz), 118.7, 84.2, 73.5, 70.7, 67.3, 67.0, 61.3, 37.6, 20.8, 20.7, 20.4, 20.0, 5.4 (*J*<sub>Pt</sub> = 508 Hz), −6.3 (*J*<sub>Pt</sub> = 659 Hz), −6.6 (*J*<sub>Pt</sub> = 658 Hz). <sup>195</sup>Pt NMR, CD<sub>3</sub>OD, δ: −2789. Anal. Calcd (found): (C<sub>34</sub>H<sub>42</sub>F<sub>3</sub>N<sub>4</sub>O<sub>12</sub>PtS): C, 41.59 (41.75); H, 4.21 (4.10); N, 5.71 (5.83).

**Synthesis of 2Pt–Glu–dep.** The same procedure as above was adopted using methanol instead of acetone. The complex was purified by recrystallization from methanol/diethyl ether (yield 94%). <sup>1</sup>H NMR, CD<sub>3</sub>OD, δ: 9.42 (m, 2H, H-2 phen and H-9 phen), 8.87 (m, 2H, H-4 and H-7 phen), 8.27 (s, 2H, H-5 and H-6 phen), 8.19 (dd, 1H, H-3 or H-8 phen), 8.14 (dd, 1H, H-8 and H-3 phen), 7.28 (d, 1H, H-4 or H-5 imidazole), 7.09 (d, 1H, H-5 or H-4 imidazole), 4.86 (d, 1H, *J*<sub>H1–H2</sub> = 6.3 Hz, H-1 glucose), 3.63 (m, 1H, H-6 glucose), 3.49 (m, 1H, H-6′ glucose), 3.59 (s, 3H, Me imidazole), 3.25 (app t, 2H, H-2 and H-4 glucose), 2.71 (t, 1H, H-3 glucose), 2.66 (m, 1H, H-5 glucose), 1.46 (s, 3H, <sup>2</sup>*J*<sub>Pt–H</sub> = 69 Hz), 1.42 (s, 3H, <sup>2</sup>*J*<sub>Pt–H</sub> = 69 Hz), 0.03 (s, 3H, <sup>2</sup>*J*<sub>Pt–H</sub> = 53 Hz). <sup>13</sup>C NMR, CD<sub>3</sub>OD, δ: 170.8 (*J*<sub>Pt</sub> = 645 Hz), 148.9, 148.5, 146.1, 139.2, 139.1, 138.5, 131.9, 131.7, 128.0, 127.8, 126.2, 125.6, 124.4, 121.1 (q *J*<sub>C–F</sub> = 322 Hz), 118.3, 85.8, 78.9, 76.5, 72.1, 68.9, 60.8, 36.8, 3.7 (*J*<sub>Pt</sub> = 511 Hz), −7.1 (*J*<sub>Pt</sub> = 663 Hz), −7.4 (*J*<sub>Pt</sub> = 663 Hz). <sup>195</sup>Pt NMR, CD<sub>3</sub>OD, δ: −2777. Anal. Calcd (found): (C<sub>26</sub>H<sub>33</sub>F<sub>3</sub>N<sub>4</sub>O<sub>8</sub>PtS): C, 38.38 (38.12); H, 4.09 (4.19); N, 6.89 (6.67).

**X-ray Crystallography.** Single crystals of **2Pt–Gal** were obtained under slow diffusion of diethyl ether stratified on a dichloromethane solution of the complex at room temperature. Data were measured at room temperature using a Bruker-Nonius KappaCCD four-circle diffractometer (graphite monochromated Mo K $\alpha$  radiation,  $\lambda$  =

0.71073 Å, CCD rotation images, thick slices,  $\phi$  and  $\omega$  scans to fill the asymmetric unit). It was not possible to collect data at low temperatures because crystals easily break under the cold N<sub>2</sub> flux of the cryostream apparatus. The reduction of data and the semi-empirical absorption correction were done using the SADABS program.<sup>50</sup> The structure was solved by direct methods (SIR97 program<sup>51</sup>) and refined by the full-matrix least-squares method on  $F^2$  using the SHELXL-2018/3 program<sup>52</sup> with the aid of the program WinGX.<sup>53</sup> Anisotropic parameters were used for non-H atoms. All the H atoms were generated stereochemically and refined accordingly to the riding model with C–H distances in the range of 0.93–0.98 Å and  $U_{\text{iso}}(\text{H})$  equal to  $1.2 \cdot U_{\text{eq}}$  of the carrier atom ( $1.5 \cdot U_{\text{eq}}$  for C<sub>methyl</sub>). Some acetate groups and triflate anions are affected by thermal disorder, which accounts for the rather high values of the displacement parameters. Some constraints were introduced in the last stage of the refinement to regularize the geometry and the displacement parameters using DFIX, SAME, SIMU, and DELU instructions of the SHELXL program. Disordered lattice solvent is present. It was not possible to model the disorder, and the PLATON SQUEEZE procedure was used to exclude the contribution of solvent to the structure. Details on crystal data and refinement parameters are reported in Table S1. The figures were generated using ORTEP-3<sup>53</sup> and Mercury CSD 4.2<sup>54</sup> programs.

**Spectrophotometric Measurements.** UV–visible spectra of 2Pt–Glu were collected on a Jasco V-650 UV–vis spectrophotometer at room temperature using 1 cm path length cuvettes. 2Pt–Glu was first dissolved in pure DMSO and then diluted in the selected buffers at a final concentration of 50  $\mu\text{M}$ . Spectra have been collected in 100% DMSO, in 10% DMSO/90% PBS (pH 7.4), and in 50% DMSO/50% PBS (pH 7.4) using the following setup: 240–450 nm wavelength range, 400 nm/min scanning speed, 2.0 nm bandwidth, and 1.0 nm data pitch. UV–vis measurements of 1Pt–Glu and of 2Pt–Glu with HEWL and HSA were performed by diluting the compounds' stock solutions to 50  $\mu\text{M}$  in 10% DMSO/90% PBS (pH 7.4). HEWL and HSA were added at about 17  $\mu\text{M}$  to yield a final metal/protein ratio of 3:1. Spectra were recorded over 7 days at room temperature. The same procedure was used in order to collect UV–vis spectra of ct-DNA in the presence of the two platinum compounds. A solution of 10  $\mu\text{M}$  ct-DNA was added to a 50  $\mu\text{M}$  Pt solution containing 10% DMSO/90% PBS (pH 7.4). Spectra were collected over 7 days.

Fluorescence spectra were collected on a HORIBA Fluoromax-4 spectrofluorometer at 25 °C using a 1 cm path length cuvette. ct-DNA was incubated with EtBr in a 1:50 molar ratio for 30 min at room temperature. Then, the complex was diluted in 10 mM ammonium acetate buffer at pH 7.5 up to a ct-DNA final concentration of 200  $\mu\text{M}$ . The ct-DNA–EtBr complex was then titrated with a 2Pt–Glu solution at a concentration of 15 mM, and fluorescence emission spectra were recorded at an excitation at 545 nm. The spectra were registered after an equilibration time of 5 min following each addition. The CD spectra of ct-DNA were registered from 220 to 320 nm on a Jasco J-810 spectropolarimeter at 25 °C in the presence of different amounts of 2Pt–Glu. Quartz cells with 0.1 cm path length were used. Each spectrum was obtained by averaging three scans and subtracting the contributions from the corresponding reference (10 mM ammonium acetate buffer at pH 7.5). Spectra were collected using samples obtained upon 24 h of incubation of ct-DNA with 2Pt–Glu at 1:0.5, 1:1, and 1:2 molar ratios. ct-DNA concentration was 200  $\mu\text{M}$ . Other experimental settings were as follows: 50 nm/min scan speed, 2.0 nm bandwidth, 0.2 nm resolution, 50 mdeg sensitivity, and 4 s response. The CD spectra of HSA and HEWL were registered upon a 24 h incubation in the presence of 1Pt–Glu and 2Pt–Glu at a 1:3 protein to metal molar ratio. Protein concentration was 0.10 mg/mL.

**Pt Compounds/DNA Interaction Studies by Electrospray Ionization Mass Spectrometry.** A 20 mer double strand DNA (dsDNA) was obtained by an annealing procedure starting from two complementary single-stranded DNAs (ssDNAs) with nucleotide base sequences corresponding to 3'-CCA CCC GGA CCC CGT ACC TG-5' for single strand 1 (ssDNA<sub>1</sub>) and to 3'-CAG GTA CGG GGT CCG GGT GG-5' for single strand 2 (ssDNA<sub>2</sub>). The annealing

reaction was carried out in water, mixing the single stranded oligonucleotides in an equal molar amount for 2 min at 95 °C and then cooling the mixture at room temperature for 45 min. 1Pt–Glu and 2Pt–Glu were dissolved in dimethyl sulfoxide (DMSO) (Bioshop, Burlington, ON, Canada) to a final concentration of 25 nmol/ $\mu\text{L}$ . Pt complexes were incubated with dsDNA in 10-fold molar excess at room temperature for 24 h. Sample mixtures were diluted 1:10 in 15 mM ammonium acetate buffer at pH 6.8; spectra were recorded in negative mode using a Q-ToF Premier (Waters, Milford, MA, USA) mass spectrometer. The acquisition was executed by direct injection at a 10  $\mu\text{L min}^{-1}$  flow rate spanning the  $m/z$  range from 1000 to 3000. The capillary voltage was fixed to 2.7 kV, and source and desolvation gas temperatures were set to 70 °C. Raw data were processed by MassLynx 4.1 (Waters, Milford, MA, USA) software.

**Cytotoxicity and Uptake Experiments.** Human A431 epidermoid carcinoma, murine BALB/c-3T3, and SVT2 fibroblasts were from ATCC. Human HaCaT keratinocyte cells were from Innoprot. Cells were cultured in Dulbecco's modified Eagle's medium (DMEM) (Sigma-Aldrich, St Louis, MO, USA) supplemented with 10% fetal bovine serum (HyClone), 2 mM L-glutamine, and antibiotics, all from Sigma-Aldrich, under a 5% CO<sub>2</sub> humidified atmosphere at 37 °C. To test the cytotoxicity of 2Pt–Glu and its derivatives, cells were seeded at a density of  $2.5 \times 10^3$  cells per well in 96-well plates. Twenty-four hours after seeding, increasing concentrations of compounds were added to the cells (0.1–125  $\mu\text{M}$ ). Cell viability was assessed by the MTT (3-(4,5-dimethylthiazol-2-yl)-2,5-diphenyltetrazolium bromide) assay after 48 h, as previously described.<sup>17</sup> Cell survival was expressed as the percentage of viable cells in the presence of the Pt drug compared to the controls, represented by untreated cells and cells supplemented with identical volumes of DMSO (maximum 1% final volume). Each sample was tested in three independent analyses, each carried out in triplicate. To study the uptake of Pt drugs, A431 cells were incubated for 48 h in the presence of each drug, tested at the IC<sub>50</sub> concentration. At the end of the incubation, Pt content was quantified by ICP-MS following a method previously reported.<sup>55</sup> Briefly, Pt concentration was measured with three replicates using an Agilent 7700 ICP-MS instrument (Agilent Technologies) equipped with a frequency-matching radio frequency (RF) generator and third generation Octopole Reaction System (ORS3), operating with helium gas in ORF and the following parameters: RF power: 1550 W; plasma gas flow: 14 L min<sup>-1</sup>; carrier gas flow: 0.99 L min<sup>-1</sup>; He gas flow: 4.3 mL min<sup>-1</sup>. <sup>103</sup>Rh was used as an internal standard (final concentration: 50  $\mu\text{g L}^{-1}$ ). Standard solutions have been prepared in 5% nitric acid at four different concentrations (1, 10, 50, and 100  $\mu\text{g L}^{-1}$ ).

**<sup>1</sup>H NMR In-Solution Studies.** 1Pt–Glu and 2Pt–Glu (10 mmol) were dissolved in DMSO-*d* (1 mL). The calculated volumes (60  $\mu\text{L}$ ) of the two solutions were diluted with the appropriate volume of 25 mM PBS buffer in D<sub>2</sub>O (pD 7.4) or DMSO-*d* to provide the final 1 mM concentration of the complex. Spectra were recorded at different times to evaluate the solution stability over 7 days.

Attempts of reduction were performed by adding ascorbic acid or glutathione to 2Pt–Glu to afford solutions (600  $\mu\text{L}$  of 10% DMSO-*d*/90% PBS (25 mM)) having 1 mM concentrations of the complex and 10–25 mM ascorbic acid or 2 mM glutathione. The solutions were incubated at 37 °C, and spectra were measured over time along 7 days.

The interaction with 2-deoxyguanosine monophosphate was studied by adding a dGMP solution in PBS (25 mM) to the appropriate volumes of 1Pt–Glu and 2Pt–Glu in DMSO-*d* to obtain final concentrations of 1 mM for the complexes and 4 mM for dGMP. Solutions were incubated at 37 °C, and spectra were recorded over 7 days.

**Electrochemical Studies.** Electrochemical data were obtained by cyclic voltammetry (CV) and differential pulse voltammetry (DPV) under N<sub>2</sub> at 20 °C using DMSO as solvent and [Et<sub>3</sub>MeN][BF<sub>4</sub>] (0.10 M) as supporting electrolyte. CV and DPV were performed in a three-electrode cell configuration consisting of a working glassy carbon (GC) electrode and two platinum wires as counter electrode and

quasi-reference electrode. Prior to voltammetric experiments, the working electrode was polished with alumina, rinsed twice with water and acetone, and then dried. The analytes were introduced into the cell with a concentration of 1 mM. In CV, the scanning rate was 0.01 V s<sup>-1</sup>, and in DPV, the pulse size was 0.025 V. All potentials are referred to the ferrocene/ferrocenium (Fc/Fc<sup>+</sup>) couple.

## CONCLUSION

Here, we report the first direct comparison between the biological activities of Pt compounds with different oxidation states and almost indistinguishable structural features. Despite the evident similarity, the complexes have different properties, and the Pt(IV) species have been shown to be less cytotoxic than the corresponding Pt(II) compound. The reasons of the poor activity and selectivity displayed by the Pt(IV) complex have been investigated through several techniques by evaluating the structural and stability properties, cellular uptake, and the interaction with macromolecules. Similarities and differences between the two types of complexes have been disclosed and discussed in terms of their chemical properties.

Although the set of results were collected in vitro and therefore in conditions different from the complex living systems, they constitute pieces useful for reconstructing the colorful mosaic related to understanding the mechanism of action of platinum-based agents.

## ASSOCIATED CONTENT

### Supporting Information

The Supporting Information is available free of charge at <https://pubs.acs.org/doi/10.1021/acs.inorgchem.9b03683>.

NMR spectra of the complexes, crystal data and additional molecular views, additional UV–vis and fluorescence spectra, ESI-MS data, CV and DPV voltammograms, and reduction peaks (PDF)

### Accession Codes

CCDC 1972544 contains the supplementary crystallographic data for this paper. These data can be obtained free of charge via [www.ccdc.cam.ac.uk/data\\_request/cif](http://www.ccdc.cam.ac.uk/data_request/cif), or by emailing [data\\_request@ccdc.cam.ac.uk](mailto:data_request@ccdc.cam.ac.uk), or by contacting The Cambridge Crystallographic Data Centre, 12 Union Road, Cambridge CB2 1EZ, UK; fax: +44 1223 336033.

## AUTHOR INFORMATION

### Corresponding Authors

**Daria Maria Monti** – Dipartimento di Scienze Chimiche, Università di Napoli Federico II, Complesso Universitario di Monte S. Angelo, 80126 Napoli, Italy; [orcid.org/0000-0002-1136-0576](https://orcid.org/0000-0002-1136-0576); Email: [mdmonti@unina.it](mailto:mdmonti@unina.it)

**Antonello Merlino** – Dipartimento di Scienze Chimiche, Università di Napoli Federico II, Complesso Universitario di Monte S. Angelo, 80126 Napoli, Italy; [orcid.org/0000-0002-1045-7720](https://orcid.org/0000-0002-1045-7720); Email: [antonello.merlino@unina.it](mailto:antonello.merlino@unina.it)

**Francesco Ruffo** – Dipartimento di Scienze Chimiche, Università di Napoli Federico II, Complesso Universitario di Monte S. Angelo, 80126 Napoli, Italy; CIRCC, 70126 Bari, Italy; [orcid.org/0000-0003-1624-079X](https://orcid.org/0000-0003-1624-079X); Email: [ruffo@unina.it](mailto:ruffo@unina.it)

### Authors

**Alfonso Annunziata** – Dipartimento di Scienze Chimiche, Università di Napoli Federico II, Complesso Universitario di Monte S. Angelo, 80126 Napoli, Italy

**Angela Amoresano** – Dipartimento di Scienze Chimiche, Università di Napoli Federico II, Complesso Universitario di Monte S. Angelo, 80126 Napoli, Italy

**Maria Elena Cucciolito** – Dipartimento di Scienze Chimiche, Università di Napoli Federico II, Complesso Universitario di Monte S. Angelo, 80126 Napoli, Italy; CIRCC, 70126 Bari, Italy

**Roberto Esposito** – Dipartimento di Scienze Chimiche, Università di Napoli Federico II, Complesso Universitario di Monte S. Angelo, 80126 Napoli, Italy; CIRCC, 70126 Bari, Italy; [orcid.org/0000-0002-2063-9050](https://orcid.org/0000-0002-2063-9050)

**Giarita Ferraro** – Dipartimento di Chimica Ugo Schiff, Università di Firenze, Sesto Fiorentino, Florence 50019, Italy

**Ilaria Iacobucci** – Dipartimento di Scienze Chimiche, Università di Napoli Federico II, Complesso Universitario di Monte S. Angelo, 80126 Napoli, Italy

**Paola Imbimbo** – Dipartimento di Scienze Chimiche, Università di Napoli Federico II, Complesso Universitario di Monte S. Angelo, 80126 Napoli, Italy

**Rosanna Lucignano** – Dipartimento di Scienze Chimiche, Università di Napoli Federico II, Complesso Universitario di Monte S. Angelo, 80126 Napoli, Italy

**Massimo Melchiorre** – ISUSCHEM, 60134 Napoli, Italy

**Maria Monti** – Dipartimento di Scienze Chimiche, Università di Napoli Federico II, Complesso Universitario di Monte S. Angelo, 80126 Napoli, Italy

**Chiara Scognamiglio** – Dipartimento di Scienze Chimiche, Università di Napoli Federico II, Complesso Universitario di Monte S. Angelo, 80126 Napoli, Italy

**Angela Tuzi** – Dipartimento di Scienze Chimiche, Università di Napoli Federico II, Complesso Universitario di Monte S. Angelo, 80126 Napoli, Italy

Complete contact information is available at: <https://pubs.acs.org/doi/10.1021/acs.inorgchem.9b03683>

### Notes

The authors declare no competing financial interest.

## ACKNOWLEDGMENTS

F.R. thanks MIUR for financial support (PRIN2015 - Prot. 20154X9ATP).

## REFERENCES

- (1) Zhang, P.; Sadler, P. J. Advances in the Design of Organometallic Anticancer Complexes. *J. Organomet. Chem.* **2017**, 839, 5–14.
- (2) Johnstone, T. C.; Suntharalingam, K.; Lippard, S. J. The Next Generation of Platinum Drugs: Targeted Pt(II) Agents, Nanoparticle Delivery, and Pt(IV) Prodrugs. *Chem. Rev.* **2016**, 116 (5), 3436–3486.
- (3) Alonso-de Castro, S.; Cortajarena, A. L.; López-Gallego, F.; Salassa, L. Bioorthogonal Catalytic Activation of Platinum and Ruthenium Anticancer Complexes by FAD and Flavoproteins. *Angew. Chem., Int. Ed.* **2018**, 57 (12), 3143–3147.
- (4) Kenny, R. G.; Marmion, C. J. Toward Multi-Targeted Platinum and Ruthenium Drugs—A New Paradigm in Cancer Drug Treatment Regimens. *Chem. Rev.* **2019**, 119 (2), 1058–1137.
- (5) Ceballos, J.; Schwalfenberg, M.; Karageorgis, G.; Reckzeh, E. S.; Sievers, S.; Ostermann, C.; Pahl, A.; Sellstedt, M.; Nowacki, J.; Carnero Corrales, M. A.; Wilke, J.; Laraia, L.; Tsachapalda, K.; Metz, M.; Sehr, D. A.; Brand, S.; Winkhofer, K.; Janning, P.; Ziegler, S.; Waldmann, H. Synthesis of Indomorphin Pseudo-Natural Product Inhibitors of Glucose Transporters GLUT-1 and -3. *Angew. Chem., Int. Ed.* **2019**, 58 (47), 17016–17025.

- (6) Upadhyay, A.; Gautam, S.; Ramu, V.; Kondaiah, P.; Chakravarty, A. R. Photocytotoxic Cancer Cell-Targeting Platinum(II) Complexes of Glucose-Appended Curcumin and Biotinylated 1,10-Phenanthroline. *Dalton Trans.* **2019**, 48 (47), 17556–17565.
- (7) Stilgenbauer, M.; Jayawardhana, A. M. D. S.; Datta, P.; Yue, Z.; Gray, M.; Nielsen, F.; Bowers, D. J.; Xiao, H.; Zheng, Y.-R. A Spermine-Conjugated Lipophilic Pt(IV) Prodrug Designed to Eliminate Cancer Stem Cells in Ovarian Cancer. *Chem. Commun.* **2019**, 55 (43), 6106–6109.
- (8) Gorle, A. K.; Rajaratnam, P.; Chang, C. W.; von Itzstein, M.; Berners-Price, S. J.; Farrell, N. P. Glycans as Ligands in Bioinorganic Chemistry. Probing the Interaction of a Trinuclear Platinum Anticancer Complex with Defined Monosaccharide Fragments of Heparan Sulfate. *Inorg. Chem.* **2019**, 58 (11), 7146–7155.
- (9) Cucciolo, M. E.; D'Amora, A.; De Feo, G.; Ferraro, G.; Giorgio, A.; Petruk, G.; Monti, D. M.; Merlino, A.; Ruffo, F. Five-Coordinate Platinum(II) Compounds Containing Sugar Ligands: Synthesis, Characterization, Cytotoxic Activity, and Interaction with Biological Macromolecules. *Inorg. Chem.* **2018**, 57 (6), 3133–3143.
- (10) Cucciolo, M. E.; De Luca Bossa, F.; Esposito, R.; Ferraro, G.; Iadonisi, A.; Petruk, G.; D'Elia, L.; Romanetti, C.; Traboni, S.; Tuzi, A.; Monti, D. M.; Merlino, A.; Ruffo, F. C-Glycosylation in Platinum-Based Agents: A Viable Strategy to Improve Cytotoxicity and Selectivity. *Inorg. Chem. Front.* **2018**, 5 (11), 2921–2933.
- (11) Annunziata, A.; Cucciolo, M. E.; Esposito, R.; Imbimbo, P.; Petruk, G.; Ferraro, G.; Pinto, V.; Tuzi, A.; Monti, D. M.; Merlino, A.; Ruffo, F. A Highly Efficient and Selective Antitumor Agent Based on a Glucoconjugated Carbene Platinum(II) Complex. *Dalton Trans.* **2019**, 48 (22), 7794–7800.
- (12) Annunziata, A.; Cucciolo, M. E.; Esposito, R.; Ferraro, G.; Monti, D. M.; Merlino, A.; Ruffo, F. Five-coordinate Pt(II) Compounds as Potential Anticancer Agents. *Eur. J. Inorg. Chem.* **2019** DOI: 10.1002/ejic.201900771.
- (13) Szablewski, L. Expression of Glucose Transporters in Cancers. *Biochim. Biophys. Acta, Rev. Cancer* **2013**, 1835 (2), 164–169.
- (14) Pettenuzzo, A.; Pigot, R.; Ronconi, L. Metal-Based Glycoconjugates and Their Potential in Targeted Anticancer Chemotherapy. *Metallo drugs* **2016**, 1 (1), 36–61.
- (15) Babak, M. V.; Zhi, Y.; Czarny, B.; Toh, T. B.; Hooi, L.; Chow, E. K.-H.; Ang, W. H.; Gibson, D.; Pastorin, G. Dual-Targeting Dual-Action Platinum(IV) Platform for Enhanced Anticancer Activity and Reduced Nephrotoxicity. *Angew. Chem., Int. Ed.* **2019**, 58 (24), 8109–8114.
- (16) Deo, K. M.; Sakoff, J.; Gilbert, J.; Zhang, Y.; Aldrich Wright, J. R. Synthesis, Characterisation and Potent Cytotoxicity of Unconventional Platinum(IV) Complexes with Modified Lipophilicity. *Dalton Trans.* **2019**, 48 (46), 17217–17227.
- (17) Deo, K. M.; Sakoff, J.; Gilbert, J.; Zhang, Y.; Aldrich Wright, J. R. Synthesis, Characterisation and Influence of Lipophilicity on Cellular Accumulation and Cytotoxicity of Unconventional Platinum(IV) Prodrugs as Potent Anticancer Agents. *Dalton Trans.* **2019**, 48 (46), 17228–17240.
- (18) Fang, T.; Ye, Z.; Wu, J.; Wang, H. Reprogramming Axial Ligands Facilitates the Self-Assembly of a Platinum(IV) Prodrug: Overcoming Drug Resistance and Safer *in Vivo* Delivery of Cisplatin. *Chem. Commun.* **2018**, 54 (66), 9167–9170.
- (19) Lo Re, D.; Montagner, D.; Tolan, D.; Di Sanza, C.; Iglesias, M.; Calon, A.; Giralt, E. Increased Immune Cell Infiltration in Patient-Derived Tumor Explants Treated with Traniplatin: An Original Pt(IV) pro-Drug Based on Cisplatin and Tranilast. *Chem. Commun.* **2018**, 54 (60), 8324–8327.
- (20) Rehm, T.; Rothmund, M.; Dietel, T.; Kempe, R.; Schobert, R. Synthesis, Structures and Cytotoxic Effects *in Vitro* of *Cis*- and *Trans*-[Pt<sup>IV</sup>Cl<sub>4</sub>(NHC)<sub>2</sub>] Complexes and Their Pt<sup>II</sup> Precursors. *Dalton Trans.* **2019**, 48 (43), 16358–16365.
- (21) Tan, M.-X.; Wang, Z.-F.; Qin, Q.-P.; Huang, X.-L.; Zou, B.-Q.; Liang, H. Complexes of Platinum(II/IV) with 2-Phenylpyridine Derivatives as a New Class of Promising Anti-Cancer Agents. *Inorg. Chem. Commun.* **2019**, 108, 107510.
- (22) Wang, Z.; Deng, Z.; Zhu, G. Emerging Platinum(IV) Prodrugs to Combat Cisplatin Resistance: From Isolated Cancer Cells to Tumor Microenvironment. *Dalton Trans.* **2019**, 48 (8), 2536–2544.
- (23) Kenny, R. G.; Chuah, S. W.; Crawford, A.; Marmion, C. J. Platinum(IV) Prodrugs - A Step Closer to Ehrlich's Vision?: Platinum(IV) Prodrugs - A Step Closer to Ehrlich's Vision. *Eur. J. Inorg. Chem.* **2017**, 2017 (12), 1596–1612.
- (24) Yap, S. Q.; Chin, C. F.; Hong Thng, A. H.; Pang, Y. Y.; Ho, H. K.; Ang, W. H. Finely Tuned Asymmetric Platinum(IV) Anticancer Complexes: Structure-Activity Relationship and Application as Orally Available Prodrugs. *ChemMedChem* **2017**, 12 (4), 300–311.
- (25) Gabano, E.; Ravera, M.; Zanellato, I.; Tinello, S.; Gallina, A.; Rangone, B.; Gandin, V.; Marzano, C.; Bottone, M. G.; Osella, D. An Unsymmetric Cisplatin-Based Pt(IV) Derivative Containing 2-(2-Propynyl)Octanoate: A Very Efficient Multi-Action Antitumor Prodrug Candidate. *Dalton Trans* **2017**, 46 (41), 14174–14185.
- (26) Theiner, S.; Grabarics, M.; Galvez, L.; Varbanov, H. P.; Sommerfeld, N. S.; Galanski, M.; Keppler, B. K.; Koellensperger, G. The Impact of Whole Human Blood on the Kinetic Inertness of Platinum(IV) Prodrugs - an HPLC-ICP-MS Study. *Dalton Trans.* **2018**, 47 (15), 5252–5258.
- (27) Bouché, M.; Bonnefont, A.; Achard, T.; Bellemin-Laponnaz, S. Exploring Diversity in Platinum(IV) N-Heterocyclic Carbene Complexes: Synthesis, Characterization, Reactivity and Biological Evaluation. *Dalton Trans.* **2018**, 47 (33), 11491–11502.
- (28) Curci, A.; Denora, N.; Iacobazzi, R. M.; Ditaranto, N.; Hoeschele, J. D.; Margiotta, N.; Natile, G. Synthesis, Characterization, and *in Vitro* Cytotoxicity of a Kiteplatin-Ibuprofen Pt(IV) Prodrug. *Inorg. Chim. Acta* **2018**, 472, 221–228.
- (29) Yempala, T.; Babu, T.; Karmakar, S.; Nemirovski, A.; Ishan, M.; Gandin, V.; Gibson, D. Expanding the Arsenal of Pt<sup>IV</sup> Anticancer Agents: Multi-Action Pt<sup>IV</sup> Anticancer Agents with Bioactive Ligands Possessing a Hydroxy Functional Group. *Angew. Chem., Int. Ed.* **2019**, 58 (50), 18218–18223.
- (30) Kastner, A.; Poetsch, I.; Mayr, J.; Burda, J. V.; Roller, A.; Heffeter, P.; Keppler, B. K.; Kowol, C. R. A Dogma in Doubt: Hydrolysis of Equatorial Ligands of Pt<sup>IV</sup> Complexes under Physiological Conditions. *Angew. Chem., Int. Ed.* **2019**, 58 (22), 7464–7469.
- (31) Wang, H.; Yang, X.; Zhao, C.; Wang, P. G.; Wang, X. Glucose-Conjugated Platinum(IV) Complexes as Tumor-Targeting Agents: Design, Synthesis and Biological Evaluation. *Bioorg. Med. Chem.* **2019**, 27 (8), 1639–1645.
- (32) Kostrhunova, H.; Petruzzella, E.; Gibson, D.; Kasparkova, J.; Brabec, V. An Anticancer Pt<sup>IV</sup> Prodrug That Acts by Mechanisms Involving DNA Damage and Different Epigenetic Effects. *Chem. - Eur. J.* **2019**, 25 (20), 5235–5245.
- (33) Chen, C. K. J.; Hambley, T. W. The Impact of Highly Electron Withdrawing Carboxylate Ligands on the Stability and Activity of Platinum(IV) pro-Drugs. *Inorg. Chim. Acta* **2019**, 494, 84–90.
- (34) Xu, Z.; Li, C.; Zhou, Q.; Deng, Z.; Tong, Z.; Tse, M. K.; Zhu, G. Synthesis, Cytotoxicity, and Mechanistic Investigation of Platinum(IV) Anticancer Complexes Conjugated with Poly(ADP-Ribose) Polymerase Inhibitors. *Inorg. Chem.* **2019**, 58 (23), 16279–16291.
- (35) Yao, H.; Xu, Z.; Li, C.; Tse, M.-K.; Tong, Z.; Zhu, G. Synthesis and Cytotoxic Study of a Platinum(IV) Anticancer Prodrug with Selectivity toward Luteinizing Hormone-Releasing Hormone (LHRH) Receptor-Positive Cancer Cells. *Inorg. Chem.* **2019**, 58 (16), 11076–11084.
- (36) Ravera, M.; Gabano, E.; McGlinchey, M. J.; Osella, D. A View on Multi-Action Pt(IV) Antitumor Prodrugs. *Inorg. Chim. Acta* **2019**, 492, 32–47.
- (37) Liu, F.; Dong, X.; Shi, Q.; Chen, J.; Su, W. Improving the Anticancer Activity of Platinum(IV) Prodrugs Using a Dual-Targeting Strategy with a Dichloroacetate Axial Ligand. *RSC Adv.* **2019**, 9 (39), 22240–22247.
- (38) Calvanese, L.; Cucciolo, M. E.; D'Amora, A.; D'Auria, G.; Esposito, A.; Esposito, R.; Falcigno, L.; Ruffo, F. Recognition of Prochiral Sulfides in Five-Coordinate Pt<sup>II</sup> Complexes: Prochiral

Sulfides in Five-Coordinate Pt<sup>II</sup> Complexes. *Eur. J. Inorg. Chem.* **2015**, *2015* (24), 4068–4075.

(39) Esposito, R.; Calvanese, L.; Cucciolo, M. E.; D'Auria, G.; Falcigno, L.; Fiorini, V.; Pezzella, P.; Roviello, G.; Stagni, S.; Talarico, G.; Ruffo, F. Oxidative Coupling of Imino, Amide Platinum(II) Complexes Yields Highly Conjugated Blue Dimers. *Organometallics* **2017**, *36* (2), 384–390.

(40) Baquero, E. A.; Flores, J. C.; Perles, J.; Gómez-Sal, P.; de Jesús, E. Water-Soluble Mono- and Dimethyl N-Heterocyclic Carbene Platinum(II) Complexes: Synthesis and Reactivity. *Organometallics* **2014**, *33* (19), 5470–5482.

(41) Astakhov, A. V.; Khazipov, O. V.; Degtyareva, E. S.; Khrustalev, V. N.; Chernyshev, V. M.; Ananikov, V. P. Facile Hydrolysis of Nickel(II) Complexes with N-Heterocyclic Carbene Ligands. *Organometallics* **2015**, *34* (24), 5759–5766.

(42) Li, D.; Ollevier, T. Mechanism Studies of Oxidation and Hydrolysis of Cu(I)-NHC and Ag-NHC in Solution under Air. *J. Organomet. Chem.* **2020**, *906*, 121025.

(43) Wexselblatt, E.; Gibson, D. What Do We Know about the Reduction of Pt(IV) pro-Drugs. *J. Inorg. Biochem.* **2012**, *117*, 220–229.

(44) Albano, V. G.; Monari, M.; Orabona, I.; Panunzi, A.; Roviello, G.; Ruffo, F. Synthesis and Characterization of Trigonal-Bipyramidal Platinum(II) Olefin Complexes with Chalcogenide Ligands in Axial Positions. X-Ray Molecular Structures of [Pt(SMe)<sub>2</sub>(Dmphen)-(Diphenyl Fumarate)], Its Cationic Dipositive Derivative [Pt-(SMe)<sub>2</sub>(Dmphen)(Diphenyl Fumarate)][BF<sub>4</sub>]<sub>2</sub>, and Free Diphenyl Fumarate. *Organometallics* **2003**, *22* (6), 1223–1230.

(45) Zhang, J. Z.; Wexselblatt, E.; Hambley, T. W.; Gibson, D. Pt(IV) Analogs of Oxaliplatin That Do Not Follow the Expected Correlation between Electrochemical Reduction Potential and Rate of Reduction by Ascorbate. *Chem. Commun.* **2012**, *48* (6), 847–849.

(46) Escolà, A.; Crespo, M.; López, C.; Quirante, J.; Jayaraman, A.; Polat, I. H.; Badía, J.; Baldomà, L.; Cascante, M. On the Stability and Biological Behavior of Cyclometallated Pt(IV) Complexes with Halido and Aryl Ligands in the Axial Positions. *Bioorg. Med. Chem.* **2016**, *24* (22), 5804–5815.

(47) Aye, K.-T.; Canty, A. J.; Crespo, M.; Puddephatt, R. J.; Scott, J. D.; Watson, A. A. Alkyl Halide Transfer from Palladium(IV) to Platinum(II) and a Study of Reactivity, Selectivity, and Mechanism in This and Related Reactions. *Organometallics* **1989**, *8* (6), 1518–1522.

(48) Nishioka, T.; Shibata, T.; Kinoshita, I. Sugar-Incorporated N-Heterocyclic Carbene Complexes. *Organometallics* **2007**, *26* (5), 1126–1128.

(49) Cucciolo, M. E.; Trinchillo, M.; Iannitti, R.; Palumbo, R.; Tesaro, D.; Tuzi, A.; Ruffo, F.; D'Amora, A. Sugar-Incorporated N-Heterocyclic-Carbene-Containing Gold(I) Complexes: Synthesis, Characterization, and Cytotoxic Evaluation: Sugar-Incorporated N-Heterocyclic-Carbene-Containing Gold(I) Complexes: Synthesis, Characterization, and Cytotoxic Evaluation. *Eur. J. Inorg. Chem.* **2017**, *2017* (42), 4955–4961.

(50) *SADABS User Manual*; Bruker Nonius BV: Delft, The Netherlands, 2002.

(51) Altomare, A.; Burla, M. C.; Camalli, M.; Casciaro, G. L.; Giacovazzo, C.; Guagliardi, A.; Moliterni, A. G. G.; Polidori, G.; Spagna, R. *SIR 97*: A New Tool for Crystal Structure Determination and Refinement. *J. Appl. Crystallogr.* **1999**, *32* (1), 115–119.

(52) Sheldrick, G. M. Crystal Structure Refinement with *SHELXL*. *Acta Crystallogr., Sect. C: Struct. Chem.* **2015**, *71* (1), 3–8.

(53) Farrugia, L. J. *WinGX* and *ORTEP for Windows*: An Update. *J. Appl. Crystallogr.* **2012**, *45* (4), 849–854.

(54) Macrae, C. F.; Bruno, I. J.; Chisholm, J. A.; Edgington, P. R.; McCabe, P.; Pidcock, E.; Rodriguez-Monge, L.; Taylor, R.; van de Streek, J.; Wood, P. A. *Mercury CSD 2.0* - New Features for the Visualization and Investigation of Crystal Structures. *J. Appl. Crystallogr.* **2008**, *41* (2), 466–470.

(55) Pontillo, N.; Pane, F.; Messori, L.; Amoresano, A.; Merlino, A. Cisplatin Encapsulation within a Ferritin Nanocage: A High-

Resolution Crystallographic Study. *Chem. Commun.* **2016**, *52* (22), 4136–4139.